

NUMERICAL ANALYSIS OF HARBOR OSCILLATION IN HARBORS OF VARIOUS SHAPES

Taro Kakinuma¹, Taishi Toyofuku², and Taisuke Inoue³

Abstract

A numerical model based on nonlinear shallow water equations is applied to study oscillations in harbors of various shapes including L-type harbors, I-type harbors with a narrowed area, a C-type harbor, a T-type harbor, and I-type harbors with a seabed crest or trough. The second mode shows a higher amplification factor at the head of an L-type harbor as its bending position is nearer to the harbor mouth. As a narrowed area of an I-type harbor is located nearer to the harbor mouth, amplification factors of the first and second modes at the harbor head are lower and higher, respectively. A C-type harbor shows rather complicated amplification because the phase difference between waves propagating through two harbor mouths depends on the position inside the harbor. The oscillation in an actual bay, i.e., Urauchi Bay, which has a shape similar to that of a T-type harbor, is also numerically simulated; damping processes are compared between Urauchi Bay and a T-type harbor.

Key words: harbor oscillation, secondary undulation, amplification factor, nonlinear shallow water equations

1. Introduction

Water oscillation in harbors of various shapes has been studied through linear theories (*e.g.* Hwang and Tuck, 1970) and hydraulic experiments (*e.g.* Horikawa et al., 1969). Numerical models have been also utilized; for example Derun et al. (2003) studied harbor oscillations in L-, F-, T-, and Y-types of harbors, where the still water depth is uniform, using a set of equations considering strong nonlinearity and strong dispersion of waves.

In the present study, a numerical model based on nonlinear shallow water equations is applied to study oscillation in harbors of various shapes including L-type harbors, I-type harbors with a narrowed area, a C-type harbor, a T-type harbor, and I-type harbors where the still water depth is distributed. The oscillation in an actual bay is also simulated, where the bay shape is similar to that of a T-type harbor with two heads and several fishing ports have been damaged by large water oscillation due to secondary undulation.

2. Numerical Calculation Method

The fundamental equations are the following nonlinear shallow water equations:

$$\frac{\partial \eta}{\partial t} + \frac{\partial}{\partial x} \{(\eta + h)U\} + \frac{\partial}{\partial y} \{(\eta + h)V\} = 0, \quad (1)$$

$$\frac{\partial U}{\partial t} + \frac{\partial U^2}{\partial x} + \frac{\partial(UV)}{\partial y} = fV - g \frac{\partial \eta}{\partial x} + A_h \left(\frac{\partial^2 U}{\partial x^2} + \frac{\partial^2 U}{\partial y^2} \right) - \frac{KU \sqrt{U^2 + V^2}}{\eta + h}, \quad (2)$$

$$\frac{\partial V}{\partial t} + \frac{\partial(UV)}{\partial x} + \frac{\partial V^2}{\partial y} = -fU - g \frac{\partial \eta}{\partial y} + A_h \left(\frac{\partial^2 V}{\partial x^2} + \frac{\partial^2 V}{\partial y^2} \right) - \frac{KV \sqrt{U^2 + V^2}}{\eta + h}, \quad (3)$$

¹Dept. of Ocean Civil Eng., Graduate School of Science and Eng., Kagoshima University, 1-21-40 Korimoto, Kagoshima, Kagoshima 890-0065, Japan. taro@oce.kagoshima-u.ac.jp

²Kyutetsu Co. Ltd., 3-12-10 Komorie, Moji, Kitakyushu, Fukuoka 800-0007, Japan. gmjhh255@yahoo.co.jp

³Dept. of Ocean Civil Eng., Graduate School of Science and Eng., Kagoshima University, 1-21-40 Korimoto, Kagoshima, Kagoshima 890-0065, Japan. taisuke02092000@yahoo.co.jp

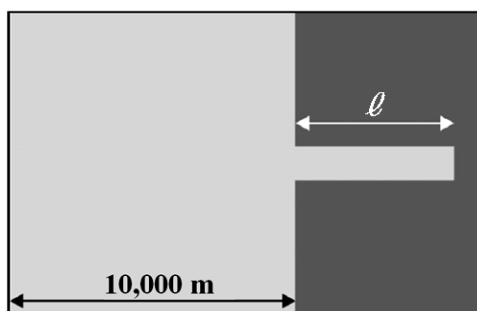


Figure 1. Computational domain for calculation of oscillation in an I-type harbor.

where U and V are horizontal velocities; η , h , f , and g are the water surface displacement, still water depth, Coriolis coefficient, and gravitational acceleration, respectively; A_h and K are factors of horizontal dissipation on and bottom friction, respectively, where $f=0.0 \text{ s}^{-1}$, $g=9.8 \text{ m/s}^2$, $A_h=3.0 \text{ m}^2/\text{s}$, and $K=0.0026$.

The fundamental equations (1) – (3) are solved using a finite difference method. The radiation condition is adopted on both incident-wave boundaries and boundaries in water areas, whereas boundaries between land and sea are assumed to be perfect-reflection walls. In each case, trains of regular waves are input on an offshore boundary, which is not a harbor mouth. The incident waves have the same wave height of 0.2 m but different wave periods. The incident wave direction is perpendicular to the cross section of a harbor mouth.

For example, an I-type harbor is shown in Figure 1, where the left-hand side of the computational domain is an incident-wave boundary. Waves propagate across the area outside the I-type harbor, after which they enter the harbor, resulting in harbor oscillation.

3. Shapes of Model Harbors and an Actual Bay

3.1. Model harbors

The following five types of model harbors are treated in the present paper.

(a) *L-type harbors with different bending positions* are shown in Figure 2, where the harbor-axis length ℓ is the same but their bending positions are different. The still water depth is 20 m in the computational domain.

(b) *I-type harbors with a narrowed area* are shown in Figure 3, where the position of or the harbor width at the narrowed areas are different. The still water depth is 20 m in the computational domain.

(c) *A C-type harbor* is shown in Figure 4, where two I-type harbors are connected with a rectangular-section channel. This type of harbor has two harbor mouths. The still water depth is 20 m in the computational domain.

(d) *I-type harbors with a seabed crest or trough* do not have uniform water depth, where the still water depth is 10.5 or 29.5 m at the longitudinal center of harbor, respectively, and the harbor bottom is uniformly sloping towards the harbor head and mouth. The still water depth at both the head and mouth of the harbors is 20 m. It should be noted that the average of still water depth is different between these two harbors. The still water depth is 20 m outside the harbors. The length and width of the harbors are 2,000 and 400 m, respectively.

(e) *A T-type harbor* has two harbor heads as shown in Figure 5, where I- and L-type harbors are also shown for comparison. The harbor width is 600 m and the still water depth is 20 m in their computational domains.

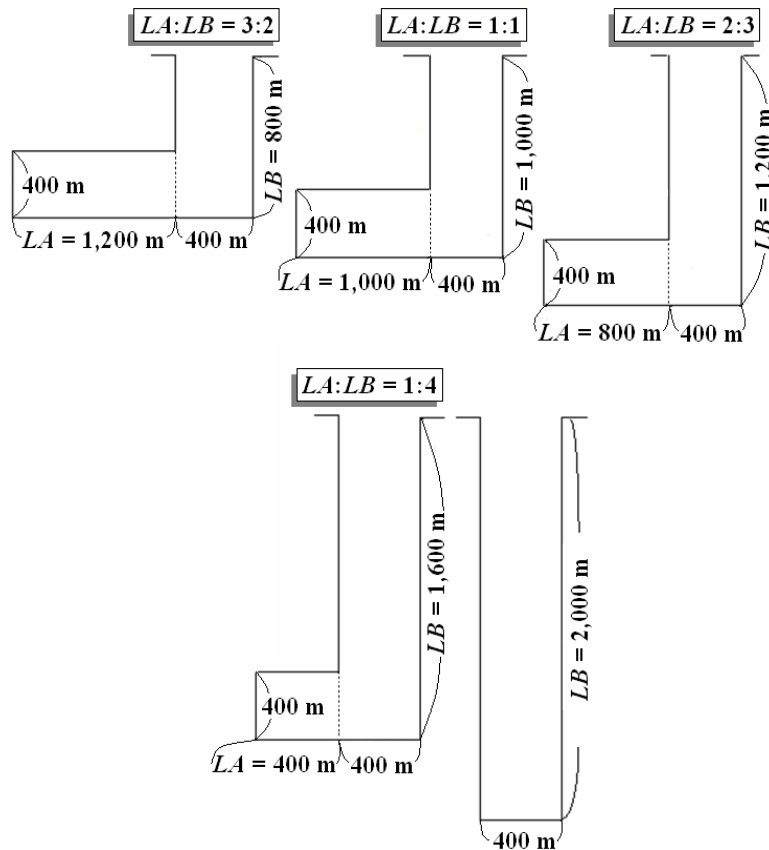


Figure 2. L-type harbors with different bending positions.

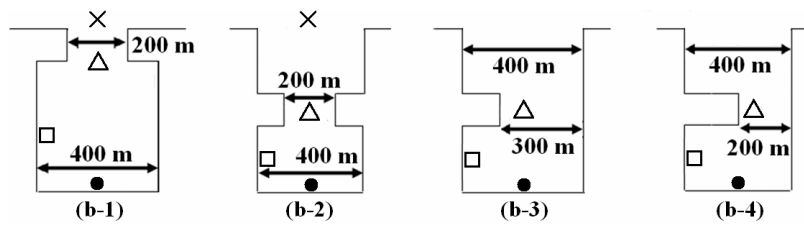


Figure 3. I-type harbors with a narrowed area.

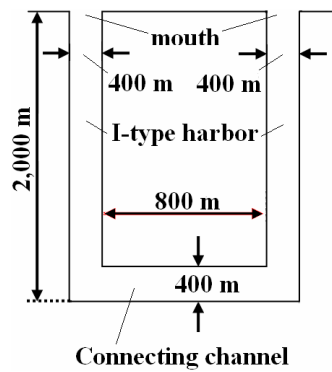


Figure 4. C-type harbor.

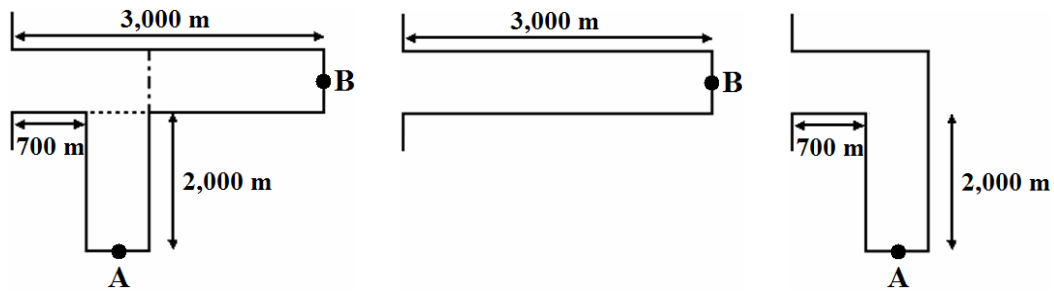


Figure 5. T-type harbor (the left-hand side), which contains an I-type harbor (the middle) or an L-type harbor (the right-hand side) as a part.

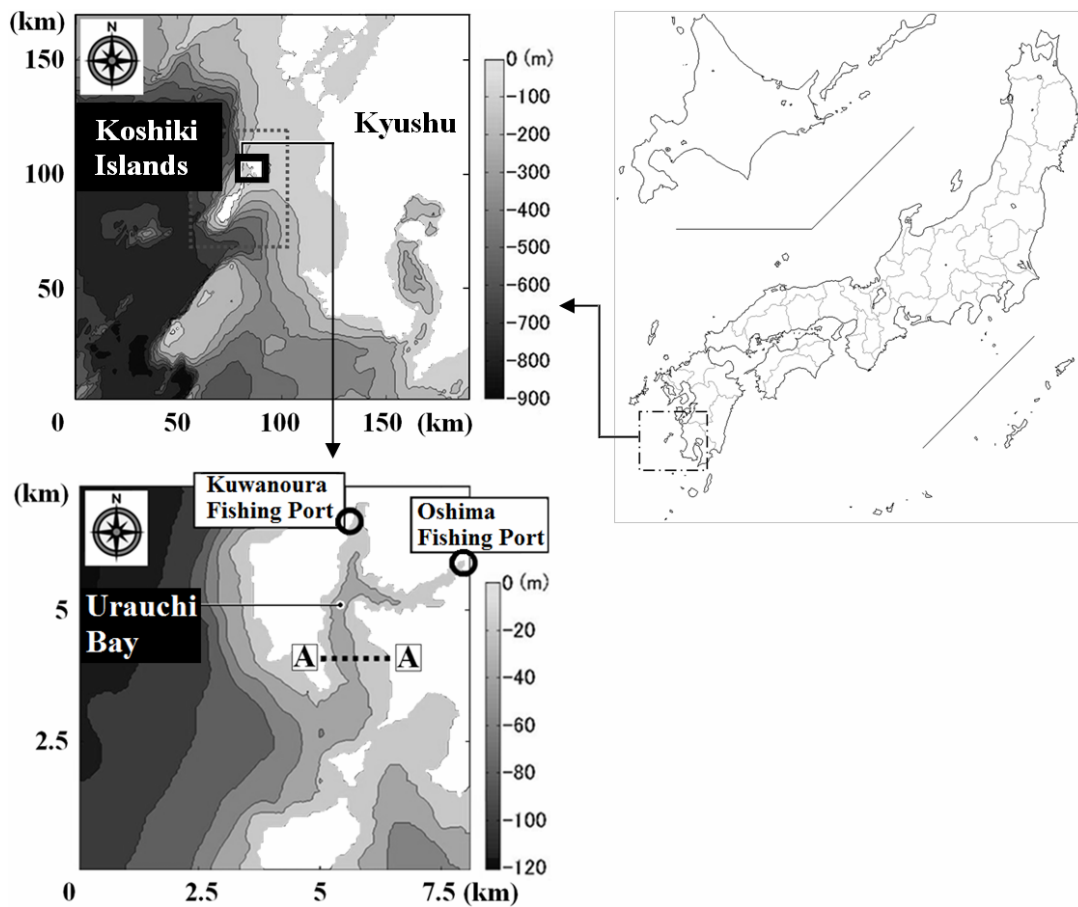


Figure 6. Urauchi Bay, Koshiki Islands including Kamikoshiki Island, Kagoshima, Japan.

3.2. Actual bay

Urauchi Bay of Kamikoshiki Island, which is situated in the western offing of Kyushu Island, Japan, has a shape similar to that of a T-type harbor. The water depth around and inside Urauchi Bay is shown in Figure 6. This bay has two bay heads and there are two fishing ports, i.e., Oshima and Kuwanoura Fishing Ports; the former is located at one bay head, while the latter is located at a point in another branch but not at another bay head.

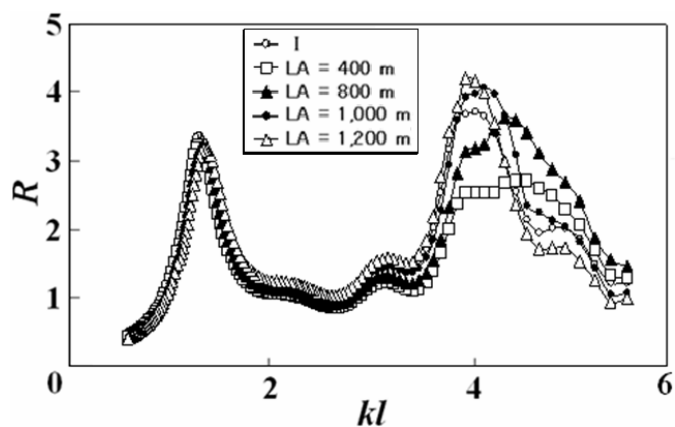


Figure 7. Amplification factors at heads of the I-type harbor and the L-type harbors with different bending positions.

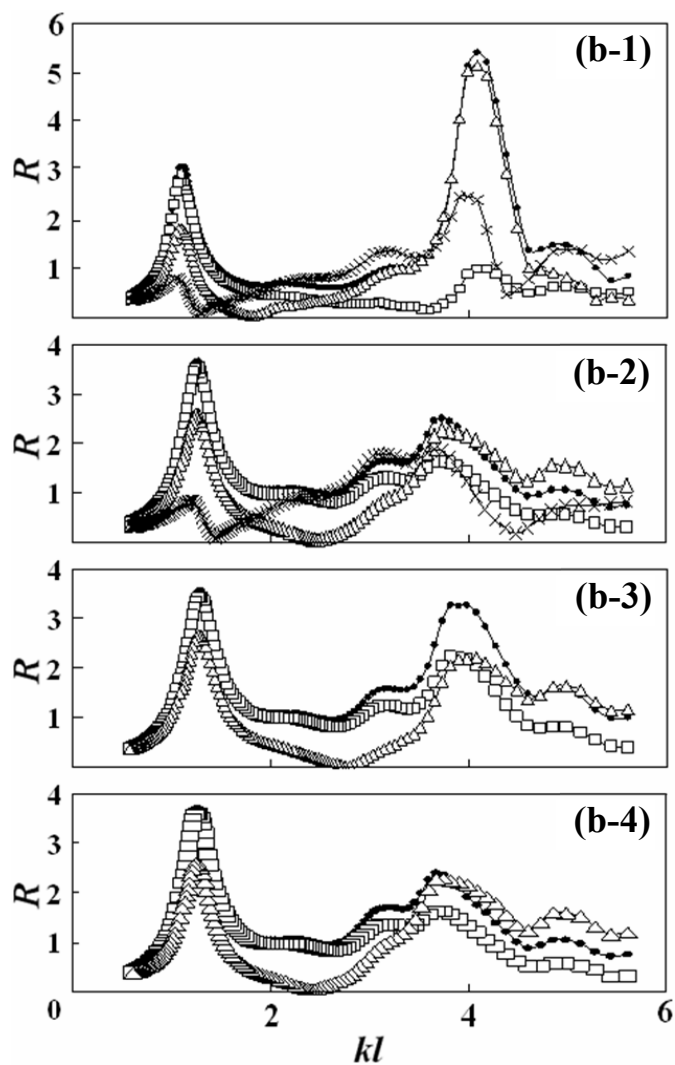


Figure 8. Amplification factors in the I-type harbors with a narrowed area. Each line shows the amplification factor at the point indicated in Figure 3 with the same symbol as used in Figure 8.

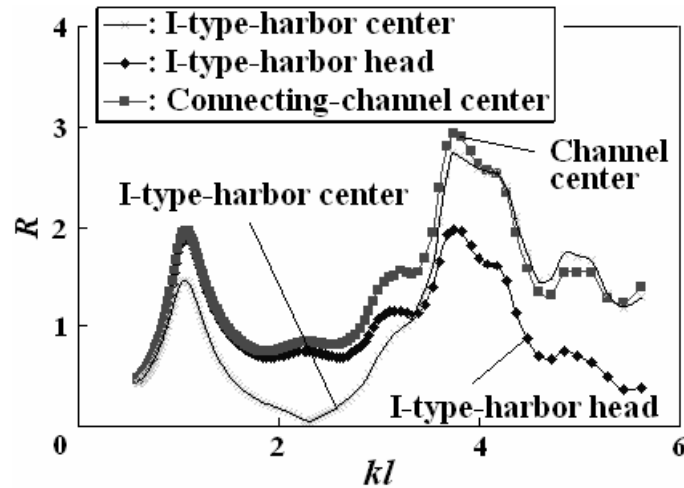


Figure 9. Amplification factors in the C-type harbor.

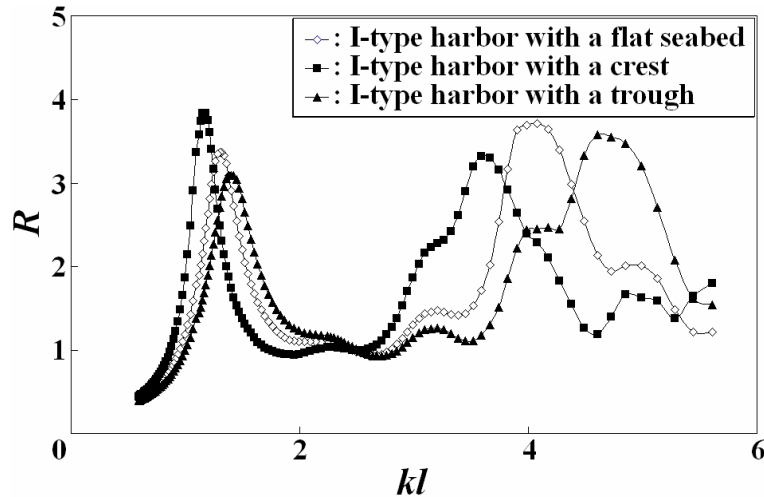


Figure 10. Amplification factors at heads of the I-type harbors with a seabed crest or trough.

4. Amplification Factors of Model Harbors

Numerical calculation results of amplification factors are discussed, where the amplification factor R is defined by the ratio of response height at each point over the incident wave height, i.e., 0.2 m, for the model harbors (a) – (d), while the amplification factor R_m is defined by the ratio of response height at each point over the response height at the harbor mouth for the model harbor (e) and the actual bay.

(a) L-type harbors with different bending positions: Figure 7 shows the amplification factor R at the heads of the harbors introduced in Figure 2, where kl is the dimensionless wave number, i.e., $kl = 2\pi\ell / (T\sqrt{gh})$. The second modes show higher R as the bending position is nearer to the harbor mouth; at the heads, the factor R is larger when $LA = 1,000$ and $1,200$ m than that of the I-type harbor.

(b) I-type harbors with a narrowed area: Figure 8 shows the amplification factor R in the harbors introduced in Figure 3. The factor R at the head for the first mode is lower in Harbor (b-1), where the narrowed area is placed at the harbor mouth, than that in Harbor (b-2), whereas the second mode shows the contrary phenomenon. The amplification factor R at the head for the second mode is lower in Harbor (b-4) than that in Harbor (b-3), where the harbor width at the narrowed area is wider than that in Harbor (b-4).

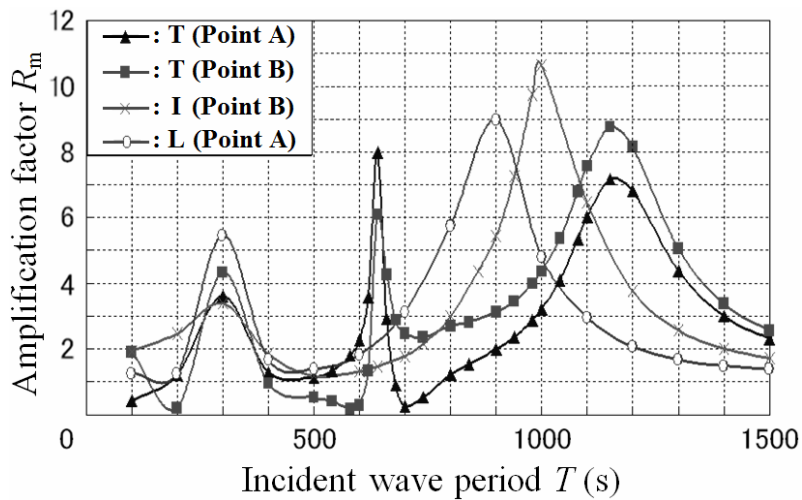


Figure 11. Amplification factors of the T-, I-, and L-type harbors at Points A and B, which are located at the harbor heads and indicated in Figure 5.

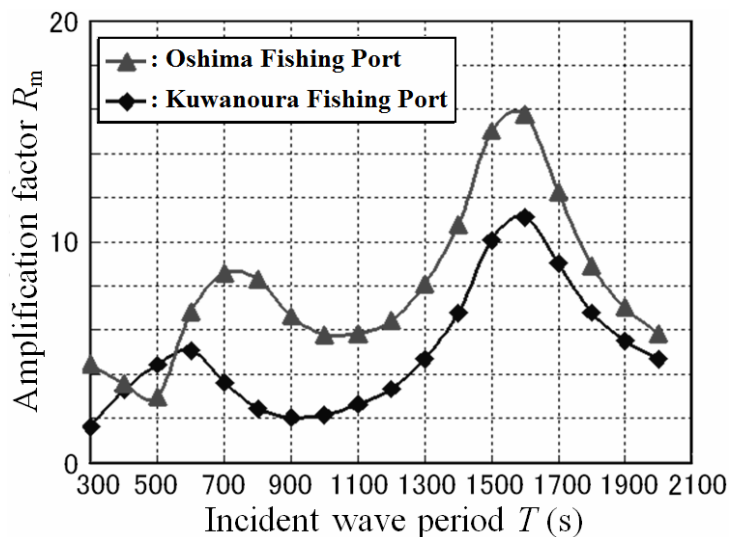


Figure 12. Amplification factors at Oshima and Kuwanoura Fishing Ports facing Urauchi Bay as shown in Figure 6.

(c) A C-type harbor: Figure 9 shows the amplification factor R in the C-type harbor introduced in Figure 4. At the heads of the I-type harbors, long waves coming through two mouths are in almost opposite phase, such that the factor R becomes lower than that at the head of the corresponding I-type harbor alone, which is shown in Figure 7. It should be noted that the phase difference between the waves through two mouths depends on the position, resulting in rather high R at the longitudinal centers of two I-type harbors, as well as the connecting channel.

(d) I-type harbors with a seabed crest or trough: Figure 10 shows the amplification factor R at the heads of the I-type harbors with a seabed crest or trough. In the I-type harbor with a seabed crest, both the first and the second modes appear at lower wave numbers than those in the I-type harbor, where the still water depth is uniformly 20 m on a flat bottom, as shown in Figure 2; another peak appears clearly when $k\ell$ is equal to about 5.0. In the I-type harbor with a seabed trough, wave numbers of both the first and the second modes become larger than those in the I-type harbor with a flat bottom.



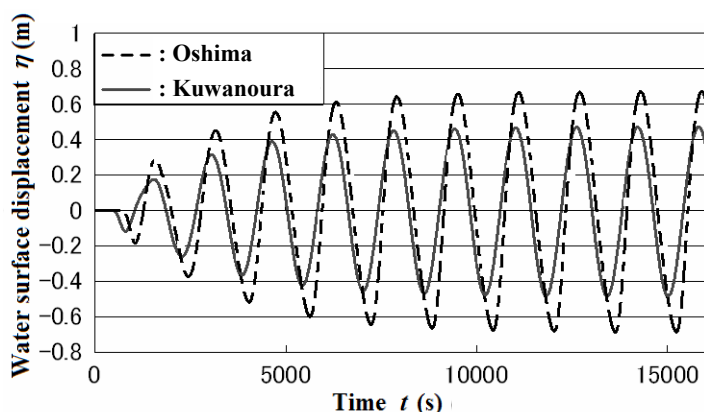
Photograph 1. Refloatation of fallen fishing boats.



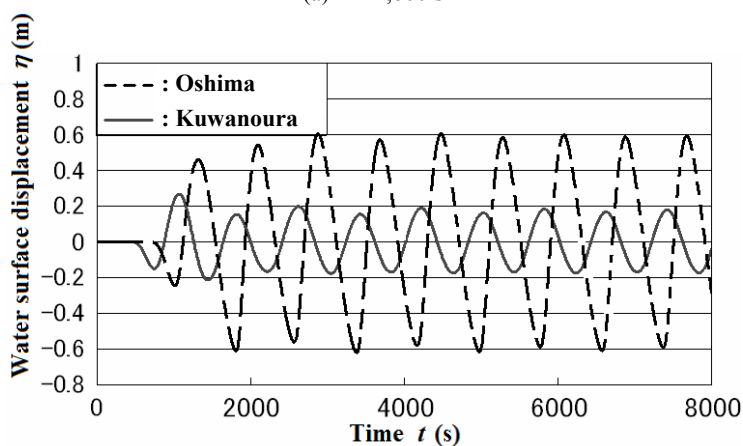
Photograph 2. Damaged fishing boat.



Photograph 3. Flooded cars.



(a) $T = 1,600$ s



(b) $T = 800$ s

Figure 13. Time variations of water surface displacements at Oshima and Kuwanoura Fishing Ports facing Urauchi Bay.

(e) *A T-type harbor*: Figure 11 shows the amplification factor R_m at harbor heads of the T-, I-, and L-type harbors introduced in Figure 5. The second mode peculiar to the T-type harbor appears as oscillation which shows antinodes at two heads of the harbor.

5. Amplification Factors of Urauchi Bay

5.1. Secondary undulation 'abiki' in Urauchi Bay

Figure 12 shows the amplification factor R_m at two fishing ports facing Urauchi Bay as shown in Figure 6. It should be noted that Oshima Fishing Port is located at a bay head, while Kuwanoura Fishing Port is located at a point in another branch but not at its head. The natural period of the first mode is about 1,600 s at both Oshima and Kuwanoura Fishing Ports; the natural period of the second mode is about 720 s at Oshima Fishing Port, while about 600 s at Kuwanoura Fishing Port.

Oshima Fishing Port has been damaged by high tides due to secondary undulation, which is called 'abiki' in Kyushu District. Rather large abiki's always occur in February or March every year. During February 24 – 26, 2009, eight fishing boats capsized at this port due to heavy abiki's superposed on a spring tide; see Photographs 1 – 3, which were taken by Satsumasendai City Office; the water level reached three meters at the present port; long waves propagated upstream on a river and overflowed nearby the residential area, such that eight houses were flooded under floor level.

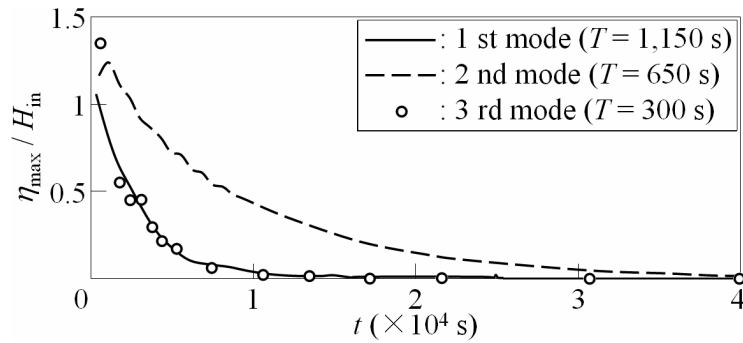


Figure 14. Time variation of the maximum height of water surface at Point A in the T-type harbor as shown in Figure 5 for harbor oscillation of the first, second, or third mode.

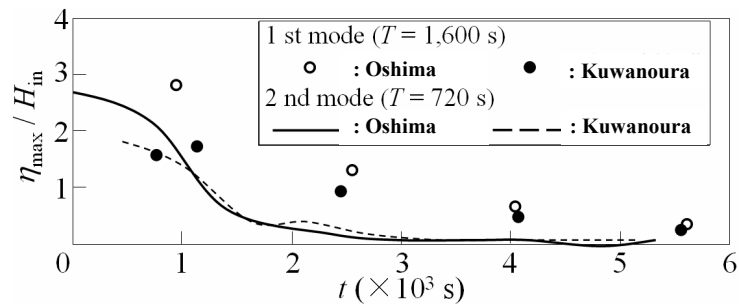


Figure 15. Time variation of the maximum height of water surface at Oshima or Kuwanoura Fishing Port facing Urauchi Bay as shown in Figure 6 for harbor oscillation of around the first or second mode.

Time variations of water surface displacements at Oshima and Kuwanoura Fishing Ports are shown in Figures 13(a) and 13(b) for around the first and second modes, respectively. According to these figures, only the oscillation around the second mode shows much phase difference between two branches, so that the first and second modes of Urauchi Bay correspond to the first and second modes of a T-type harbor, respectively.

5.2. Damping processes of oscillations in the T-type harbor and Urauchi Bay

In order to study the damping process of oscillation in the T-type harbor as shown in Figure 5, a quasi-steady state has been achieved by continuously incident waves, after which the incidence is stopped when $t = 0$ s. The period of the incident waves is the same as that of the first, second, or third mode, where the natural periods of the T-type harbor are evaluated through Figure 11.

Figure 14 shows the time variation of the maximum height of water surface at Point A, which is indicated in Figure 5, during the damping of harbor oscillation for the case of the first, second, or third mode after $t = 0$ s. When long waves enter the T-type harbor, the wave energy is partly trapped in the harbor. The mode most likely to remain in the T-type harbor is the second mode, where the long waves repeat propagation between two harbor heads.

On the other hand, Figure 15 shows the time variation of the maximum height of water surface at Oshima or Kuwanoura Fishing Port facing Urauchi Bay as shown in Figure 6. The mode which is most likely to remain in the bay is the first mode and not the second mode.

The reason why the mode most likely to remain is different between the model harbor and the actual bay is supposed as follows: 1) the width of the actual bay is not uniform, 2) the still water depth is not uniform in the actual bay, and 3) the shape of the actual bay is bended.

6. Conclusions

A numerical model based on nonlinear shallow water equations is applied to study oscillations in harbors of various shapes including L-type harbors, I-type harbors with a narrowed area, a C-type harbor, a T-type harbor, and I-type harbors with a seabed crest or trough, as well as an actual bay.

The second mode shows a higher amplification factor at the head of an L-type harbor as its bending position is nearer to the harbor mouth.

As a narrowed area of an I-type harbor is located nearer to the harbor mouth, amplification factors of the first and second modes at the harbor head are lower and higher, respectively.

A C-type harbor shows rather complicated amplification because the phase difference between waves through two harbor mouths depends on the position inside the harbor.

The oscillation in Urauchi Bay has the second mode peculiar to T-type harbors, where antinodes appear at their two harbor heads. Future work is required to make clear the reason why the damping processes are different between the model harbor and the actual bay.

Acknowledgements

Sincere gratitude is extended to Satsumasendai City Office for providing Photographs 1 – 3.

References

- Derun, A. B., Kakinuma, T., and Isobe, M., 2003. A nonlinear numerical model of harbor oscillations and its application to responses of harbors of various shapes. *Proc. Coastal Eng., JSCE*, 50: 231-235. (in Japanese)
- Horikawa, K., Shuto, N., and Nishimura, H., 1969. Characteristic oscillation of water in an L-shaped bay. *Coastal Eng. in Japan*, 12: 47-56.
- Hwang, L-S. and Tuck, E. O., 1970. On the oscillations of harbours of arbitrary shape. *J. Fluid Mech.*, 42: 447-464.